4 Structural setting

The following section documents the large-scale context of the Kucing Liar mineralisation, as reflected by the distribution of the major hydrothermal minerals. Routine logging of all drill core included identification of lithology and estimation of individual mineral abundances for all core samples (Appendix IV). During routine exploration drilling, sample intervals were assigned by mine geologists at regular lengths of 3m but made shorter where significant changes in geology were present (N. Wiwoho, pers comm.). Technicians then split the core using a screw press to produce a sample ready for assay. A short length of drill core (10-20cm) was removed from each assayed interval prior to splitting, and retained, producing an archive of “skeleton” core. The drill holes were logged in two phases from Sept.-Nov. 1997 and June-Sept. 1999. During the first phase, continuous (“full core”) that had been split for sampling was utilised, while during the second period only skeleton core was examined due to the much shorter time required to examine and log a single hole. The second period of logging revisited many of the drill holes logged on the first occasion, enabling a comparison between logs of continuous core versus skeleton core. No major differences were found comparing the data from the two different sample collections.

The structural setting has been interpreted independently for this research program from the skeleton core logged by this author to develop detailed cross sections through the mineralised zone. Polygonal outlines developed from data within individual drilling stations for major stratigraphic contacts each of the major mineral assemblages honour the position of contacts on drillhole traces and were converted into wireframes. Three-dimensional surfaces representing the major stratigraphic contacts have been derived from correlation of stratigraphy between radial drill fans (Chapter 1), and are used to illustrate the structural setting of mineralisation. Visual estimates of mineral abundances in drill core samples (see Appendix V) were also analysed in three dimensions using Vulcan and Surpac mine-environment software. Cross sections of these surfaces and isosurfaces are the primary method used to interpret structural controls on fluid flow.

4.1 STRATIGRAPHIC AND FLUID FLOW MODELLING

The main units of interest in the Kucing Liar deposit are the Ekmai and Waripi Limestones, and less importantly the Faumai Limestone, the Sirga Sandstone and the Kais Limestone. Each of these units is unique with respect to the overall sequence. Their contacts are important in identifying stratigraphical position as well as the location of fault zones. The positions of the distinctive marker horizons have been correlated between drill stations to form three-dimensional surfaces and are combined with the 3D distribution of hydrothermal alteration to provide as full a picture as possible of the structural history of the Kucing Liar system.

4.1.1 Lithological distribution

Stratigraphic sequence recognition

While the original composition and texture of wall rocks could be identified for type samples in KLS1-1 and KLS3-1, much of the sequence is affected by hydrothermal alteration. As the wall rocks in the mineralised zone are, by definition, extensively replaced, identification of texture retention during alteration is an important step in correctly assigning stratigraphic position of host rocks. Textural retention and lithological control of mineralogy is a feature of hydrothermal mineral development at Kucing Liar, which, in combination with unique sequences and marker horizons, allows stratigraphic characterisation of the altered sequences in the main mineralised zone. As the sequence of lithology has been established, deviations from the expected lithology identify the components added during modification. Each type of alteration displays a continuum of modification that can be traced from original texture and composition in KLS1-1 and KLS3-1 through to total replacement of the original rock within the mineralised zone.

Textural retention during alteration

Fundamentally, there are only three sedimentary rock types, i.e. limestone, sandstone and shale, which host Kucing Liar alteration and mineralisation, each of which can be identified either by a distinctive texture or a particular alteration mineralogy (Plate 4-1).

The base of the mineralised zone is marked by the Ekmai Sandstone which is a relatively homogeneous unit with monotonous white K-feldspar ± muscovite ± covellite ± pyrite. In some drilling, sharp contacts between K-feldspar and quartz-dominant alteration were observed. The deepest penetration of the Ekmai Sandstone (in KL42-3) intersected a section of clinopyroxene-garnet-K-feldspar-biotite hornfels that is very similar in appearance to altered sections of the Ekmai Limestone. The lower contact with the Ekmai Sandstone marks a change from underlying homogeneous sandstone to very fine-grained shale and is distinctive in altered sequences where the overlying zone is typified by a 5-10m zone of abundant green or brown-red garnet and magnetite in the lower Ekmai Limestone. The main body of the Ekmai Limestone is generally homogeneous and typified by very fine-grained hornfels that may be green (pyroxene-feldspar), white (K-feldspar) or brown (K-feldspar ± biotite). Where present, the Ekmai shale is altered to a distinctive brown K-feldspar ± biotite rock and contains a quartz stockwork that is distinct from sheeted vein arrays hosted in the underlying Ekmai Limestone and which are absent from overlying Waripi Limestone (zone 8 in Plate 4-1). This unit is not present throughout the mineralised zone, but it is definitive.

The Waripi Limestone overlies the Ekmai Limestone and typically contains a number of different zones where intersected in the deposit. The lowermost zone commonly hosts thick concentrations of magnetite or garnet that form sharp contacts with clinopyroxene-plagioclase or K-feldspar-biotite altered shale. This zone is typified by intense brecciation with an abrupt lower contact to the Ekmai Limestone and a transitional contact to overlying skarn alteration (zones 5 and 6 in Plate 4-1). The lower contact with the Ekmai Limestone represents a change from very fine-grained black shale to fine-grained grey peloid limestone and as such is easily recognised. Diopside skarn occurs above the magnetite breccia /garnet zone and has been overprinted by orange humite-forsterite, dark green phlogopite, green tremolite-actinolite or thin magnetite zones (zone 4 in Plate 4-1). The upper contact of skarn and accompanying alteration is commonly sharp, in some cases (zones 3 and 4 in Plate 4-1) defined by a thin concentration of garnet accompanied by sphalerite and galena mineralisation. A zone of calcite alteration above this contact is gradational to grey dolostone (zone 3 in Plate 4-1). This is succeeded by the upper Waripi sandstone member, which is typically intensely altered to vuggy quartz and contains metre-scale lenses of pyrite. This alteration does not typically extend outside the quartz layer, which is overlain by thin K-feldspar-biotite hornfels developed in thin shale.

Marker horizons

The precise position of the upper Waripi Limestone contact with the Faumai Limestone is difficult to recognise as the thin (~5m) laminated sandstone layer that marks the top of the Waripi Limestone is commonly not observed due to the scale of sampling (see Appendix V). However, the approximate location of the contact is indicated by the location of the much thicker (~50m) upper Waripi sandstone member and its accompanying, easily identifiable shale layer (zones 2 and 12 in Plate 4-1). The position of the Idenberg Fault Zone can be identified in many drill holes due to variation from the normal stratigraphic sequence. The Ekmai Sandstone is known from regional studies to be 600m thick (Chapter 1). Drill holes oriented from near vertical or toward the northeast either intersect thick monotonous sandstone or porphyry. However, drill holes oriented toward the southwest do not follow the expected sequence, indicating the presence of a fault. The Idenberg Fault Zone is manifested either as an abrupt change in lithology, which may be altered sandstone to altered limestone, commonly separated by 5 to 10m of magnetite ± phlogopite ± tremolite ± chalcopyrite ± pyrite, or as a broader zone characterised by fragmental rocks altered to magnetite ± quartz ± pyrite (zone 9 in Plate 4-1). In many instances the alteration mineralogy does not allow specific identification of the texture or lithology of the precursor. Garnet, magnetite, quartz and pyrite are all associated with extensive fragmentation of the host rocks (Chapter 3) and it is interpreted that intense development of these minerals indicates the presence of a fractured zone that represents the position of a fault (Plate 4-1).

Out-of sequence limestone has been encountered beneath the Ekmai Limestone on the southwest margin of the main mineralised zone. A thick magnetite zone commonly occupies the contact between normal stratigraphy and out-of-sequence limestone (zone 9 in Plate 4-1). The limestone is variably altered with increasing intensity with depth from calcite to calcite ± magnetite with minor humite development and finally to clinopyroxene and humite skarn overprinted by retrograde tremolite-actinolite and serpentine (zones 10 and 11 in Plate 4-1). The distinctive upper Waripi sandstone member is occasionally recognised in deeper drilling intersections within this zone of altered limestone from the same distinctive quartz and potassic hornfels alteration identified above the mineralised zone (e.g. zone 12 in Plate 4-1). Additionally, sandstone of similar thickness to the upper Waripi sandstone member but containing a shale layer in the middle rather than at the top is identified in a small number of holes and is interpreted to be the Sirga Sandstone. Where recognised, the Sirga Sandstone is quartz-garnet altered with minor lenses of pyrite. Recognition of these distinctive layers in deeper drilling confirms the presence of a fault zone and allows the magnitude of displacement to be measured.

Stratigraphical interpretations indicate that the Kucing Liar deposit can be divided into two parts with similar sequences separated and offset by the Idenberg Fault Zone. The position of this fault is indicated by departure from the ideal stratigraphic sequence (Figure 4-1). The rocks above the fault consist of well-constrained stratigraphic sequence of Waripi Limestone, Ekmai Limestone and Ekmai Sandstone and will be referred to as the main mineralised zone. The footwall stratigraphy is less well defined due to limited drilling. The general impression of the structure at Kucing Liar can be gained by comparing the sequences intersected at different drill stations along the strike of the system (Figure 4-1). The stratigraphy of Kucing Liar is generally consistent along strike though there is a significant change in the structure at station KL44, which marks the western extent of mineralisation (Figure 4-1). Below the fault zone the Waripi Limestone and Faumai Limestone are recognised from the relative position of a second intersection of the upper Waripi sandstone member (Figure 4-1). The Sirga Sandstone is also recognised in KL44-2 adjacent to the main mineralised zone but separated from it by a porphyry intrusion that occurs in the Idenberg Fault Zone (Figure 4-1).

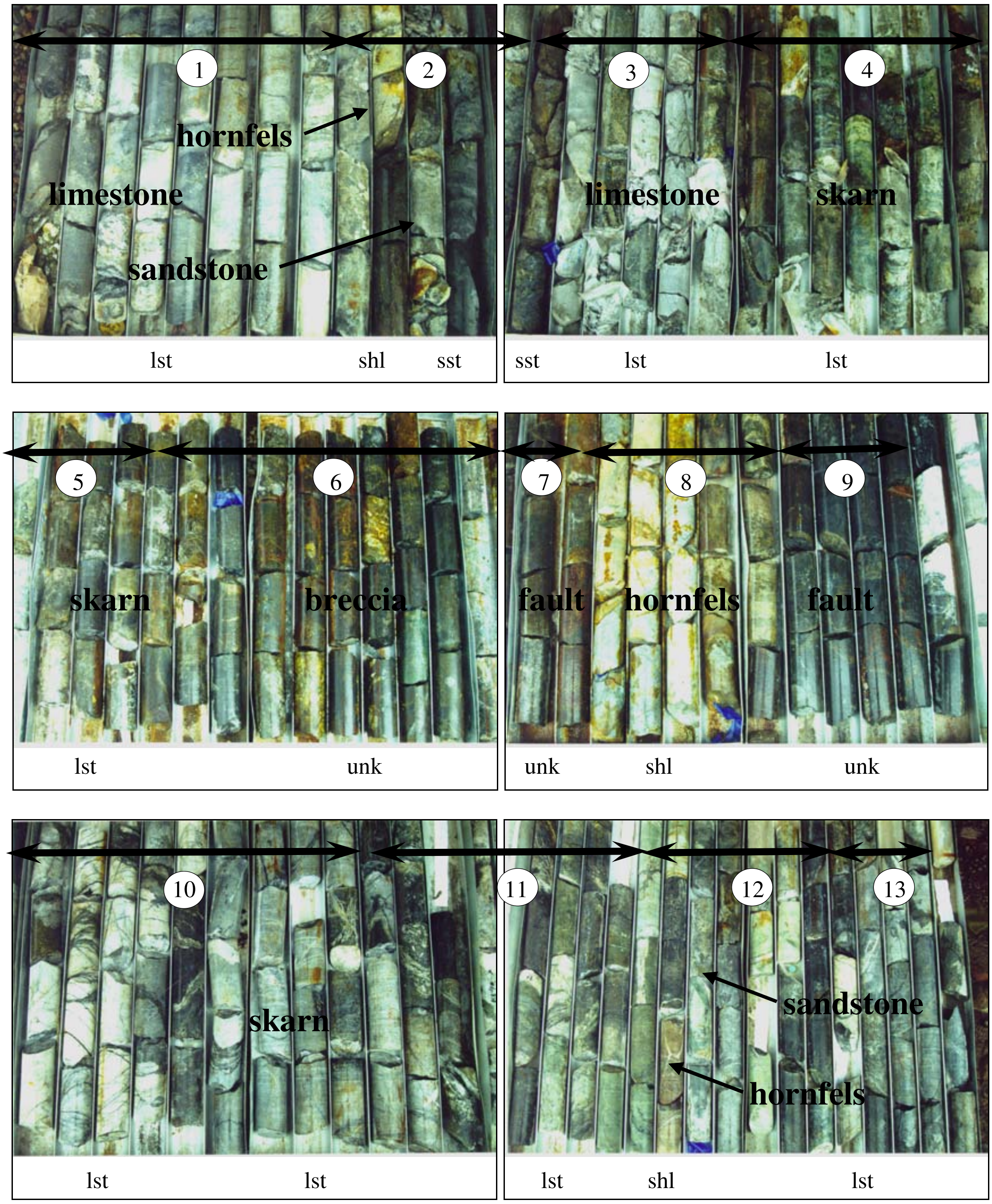

Plate 4-1 An example of lithological sequence commonly found in faulted regions

Drill core samples from KL40-07 (Figure 4-1) representing assay intervals that are generally 3m long. The total depth of the hole is 911m (lst = limestone, shl = shale, sst = sandstone, unk = unknown). Zones: 1–carbonate altered limestone, 2–quartz altered sandstone including feldspar + biotite altered shale, 3–carbonate altered limestone, 4–pyroxene-garnet-phlogopite-tremolite altered limestone, 5–pyroxene altered limestone plus magnetite-pyrite altered zones, 6–magnetite plus minor pyroxene altered limestone, 7–magnetite altered zone, 8–feldspar±biotite altered shale, 9–magnetite altered zone, 10–calcite±magnetite±humite altered limestone, 11–pyroxene altered limestone, 12–pyroxene and quartz altered sandstone including feldspar±biotite altered shale, 13–calcite-magnetite and humite-forsterite altered limestone.

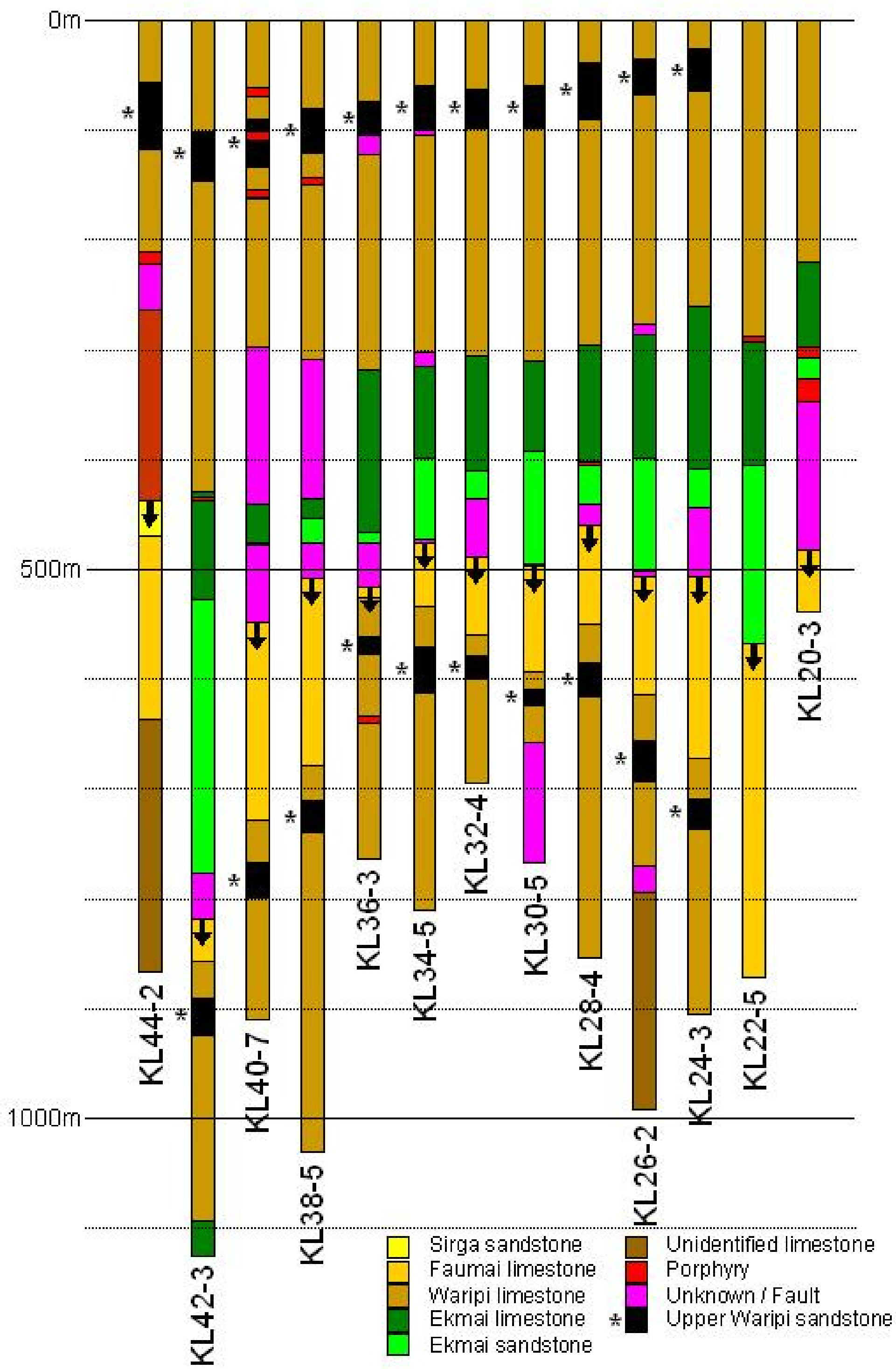

Figure 4-1 Stratigraphic patterns identified in drilling

Stratigraphic interpretation of drilling from each drill station is illustrated using holes that dip approximately 60º toward southwest, though significantly steeper holes (KL30-5, KL42-3) were included as there were no other satisfactory holes from these stations. The position of the upper Waripi sandstone member relative to the drill collars illustrates continuity of stratigraphy and the basic orientation of strike. An arrow marks the start position of out-of-sequence stratigraphy. See Appendix I for the position of each of these drill holes. There is a large amount of vertical exaggeration as the holes are spaced approximately 100m apart (see Chapter 1), meaning the holes represent 1,200m of strike length.

Large-scale geometry

The Waripi and Ekmai Limestone units, as well as upper sections of the Ekmai Sandstone, dominate the stratigraphy of the main mineralised zone northeast of the Idenberg Fault Zone (Figure 4-2, Figure 4-3). Much of the rock mass intersected on the southwest side of the Idenberg fault zone is undifferentiated limestone at higher levels, though it is likely to be the Kais Limestone, due to the local recognition of the Sirga Sandstone (Figure 4-2). However, the recognition of the upper Waripi sandstone member in much of the deeper drilling allows some reconstruction of the geometry of stratigraphy in the footwall of the Idenberg Fault Zone. Bedding strikes consistently at ~290° in this part of the system. Unit boundaries dip north but are concave upwards directly adjacent to the Grasberg Igneous Complex, which is intersected at the centre and northwest end of the deposit and has a near vertical contact with host rocks (Figure 4-3). Although data on the southwest side of the Idenberg Fault Zone are scarce, the strike of the upper Waripi shale/sandstone marker is observed to be similar to that on the northeast side. The Ekmai Limestone is thicker in the southeast than in the northwest, while the Waripi Limestone is thicker in the northwest than in the southeast (Figure 4-3). Thickening is coincident with inflections in the strike of the Ekmai Limestone. The distribution of marker horizons in cross section, especially the upper Waripi shale/sandstone marker, illustrate that total vertical separation across the Idenberg Fault Zone is ~600m, north side up relative to south (Figure 4-3). The Idenberg Fault Zone has an offset geometry when viewed in cross section, plan and long section (Figure 4-3). The 290° striking segments are 50-100m thick, while vertical, 300° striking segments are only 5-10m thick.

(Overleaf): Figure 4-2 is a series of sections of each cross section studied during this research program. They are included to demonstrate the continuity of stratigraphy as well as the variation in exposure scale for each section. The stratigraphic patterns are derived from projection of drill traces onto flat page and so may not be strictly accurate dur to non-planar drill traces. The relative position of the shale horizon marker in the upper Waripi Limestone gives an impression on the scale of displacement across the Idenberg Fault Zone. Stratigraphic unit codes are; Tngk = Kais Limestone, Tngs = Sirga Sandstone, Tngf = Faumai Limestone, Tngw = Waripi Limestone, Kkel = Ekmai Limestone, Kkes = Ekmai Sandstone. Pink shaded areas depict areas where stratigraphic assignment is not possible, while dotted pattern depicts fault breccia zones.

Figure 4-2 Serial sections of Kucing Liar lithology (refer Chapter 1 for section locations)

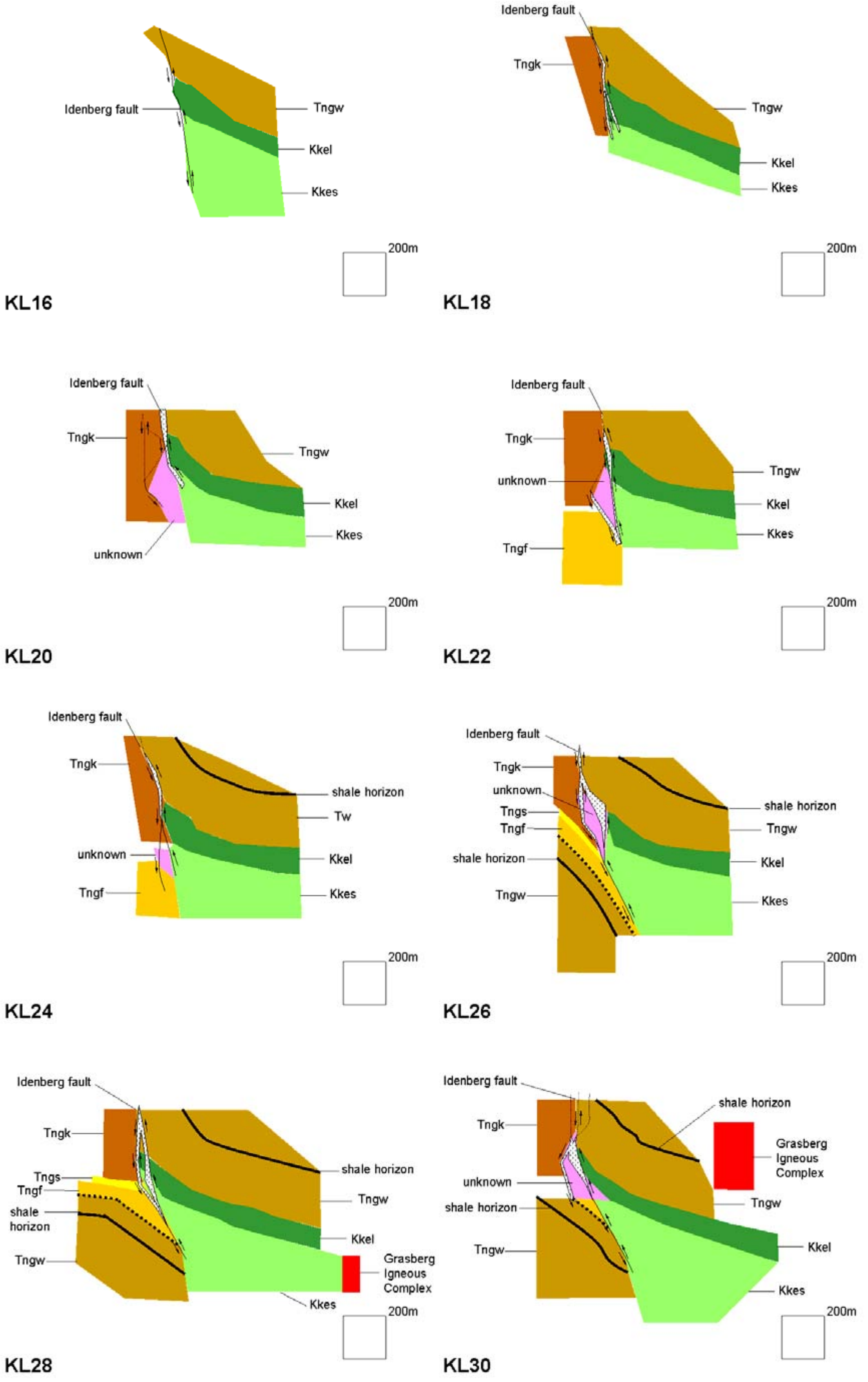

Figure 4-2 Serial sections of Kucing Liar lithology (cont.)

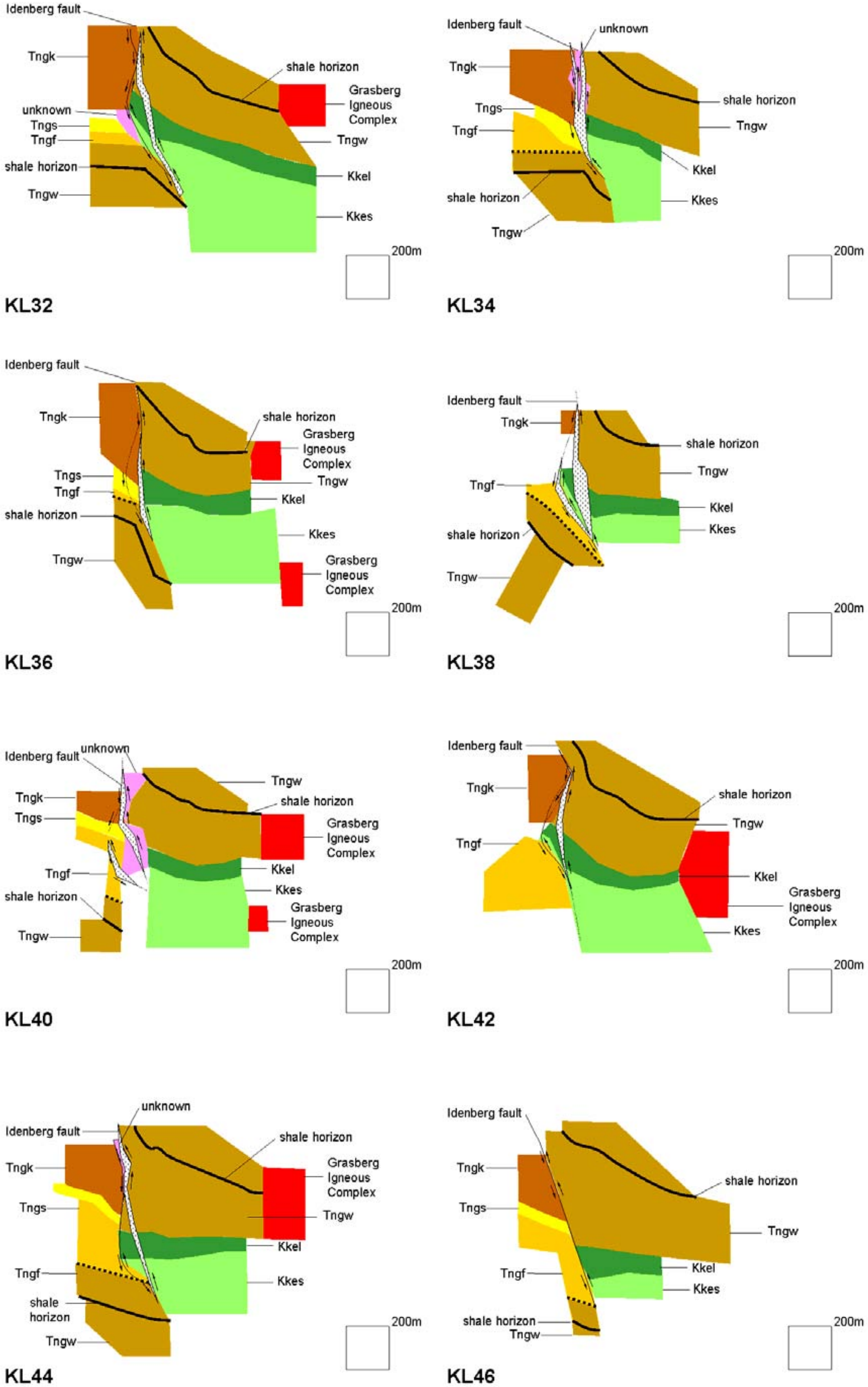

Figure 4-3 Interpretative cross sections of Kucing Liar stratigraphy from wireframes

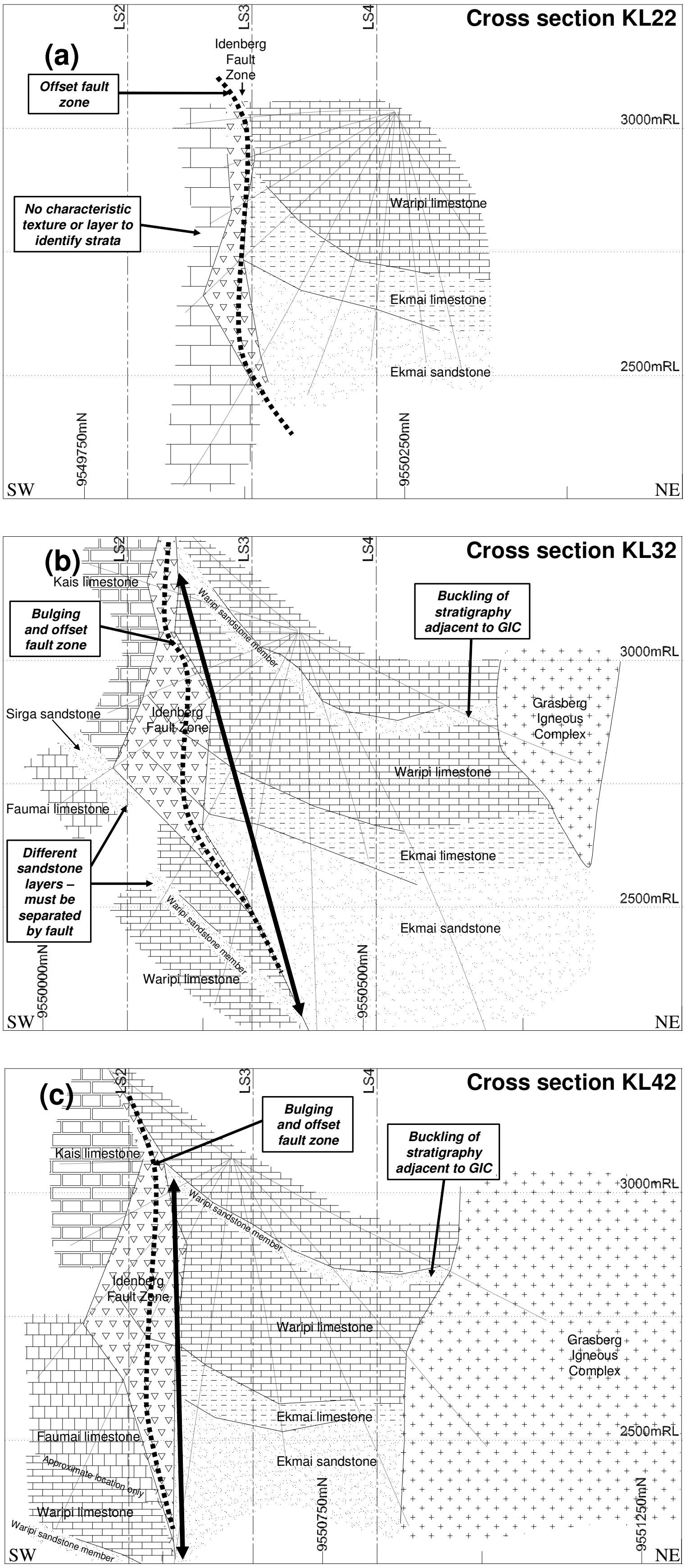

Three representative cross sections selected from the centre and either end of the deposit (spaced roughly 500m apart, see Figure 4-4). Unlike the previous Figure 4-2, the stratigraphic contacts in this figure are not projections but are sections taken from individual wireframes that were interpreted for each unit contact from its real position in each drill trace using 3D mine environment software. The drill traces are projected onto section planes as grey lines. No vertical exaggeration. (a) A cross section through station KL22 shows relatively simple stratigraphic succession adjacent to a discrete fault offset (dotted line). Due to carbonate alteration and little exposure the exact position of the stratigraphy to the left (southwest) of the Idenberg Fault Zone (IFZ) could not be determined. (b) A section through KL32 in the centre of deposit shows a much greater exposure of the system. In this section the offset in the IFZ is much more pronounced. More drilling past the IFZ has allowed identification of the upper Waripi shale-sandstone marker horizon and subsequent overall movement on the fault zone (heavy black arrow) (c) A section through KL42 again shows the IFZ offset and displacement (heavy black arrow), as well as the position of the Grasberg Igneous Complex (GIC). Note the apparent buckling of stratigraphy adjacent to the GIC.

Figure 4-4 Interpretative plan sections of Kucing Liar stratigraphy from wireframes

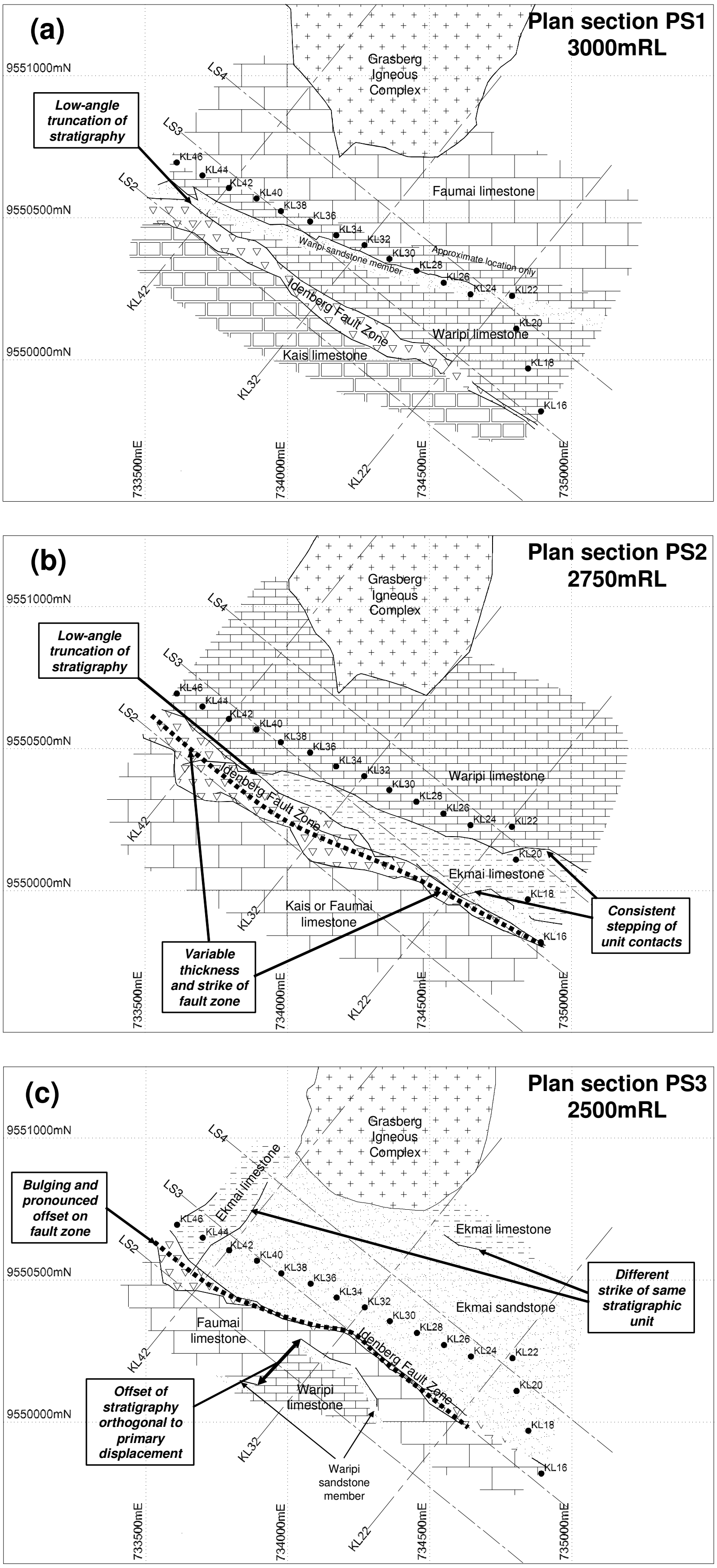

Three representative plan sections spaced 250m apart, see Figure 4-3 for locations. The stratigraphic contacts in this figure were created from individual wireframes that were interpreted from each cross section. The locations of drill stations for each cross section are projected onto the sections for orientation purposes. The outline of the Grasberg Igneous Complex (GIC) was supplied by PT Freeport Indonesia geologist Peter Manning. (a) A plan section through 3000mRL (above sea level) shows the angular relationship between sedimentary units and the Idenberg Fault Zone (IFZ).The IFZ in this section is relatively simple. The sandstone-shale marker horizon in the Upper Waripi Limestone is shown intersecting the IFZ in the far west. (b) A section through 2750mRL (above sea level) shows the truncation of the Ekmai Limestone against the IFZ. Also apparent in the east are offsets in the Ekmai Limestone that may be an expression of minor faulting associated with the IFZ. The IFZ shows variable thickness and orientation in this section. (c) A plan at 2500mRL (a.s.l.) shows a complicated orientation of the Ekmai Limestone and a very narrow but offset IFZ. This section also indicates an offset of the stratigraphy in the footwall of the IFZ which is normal to the main fault zone.

Figure 4-5 Interpretative longitudinal sections of Kucing Liar stratigraphy from wireframes

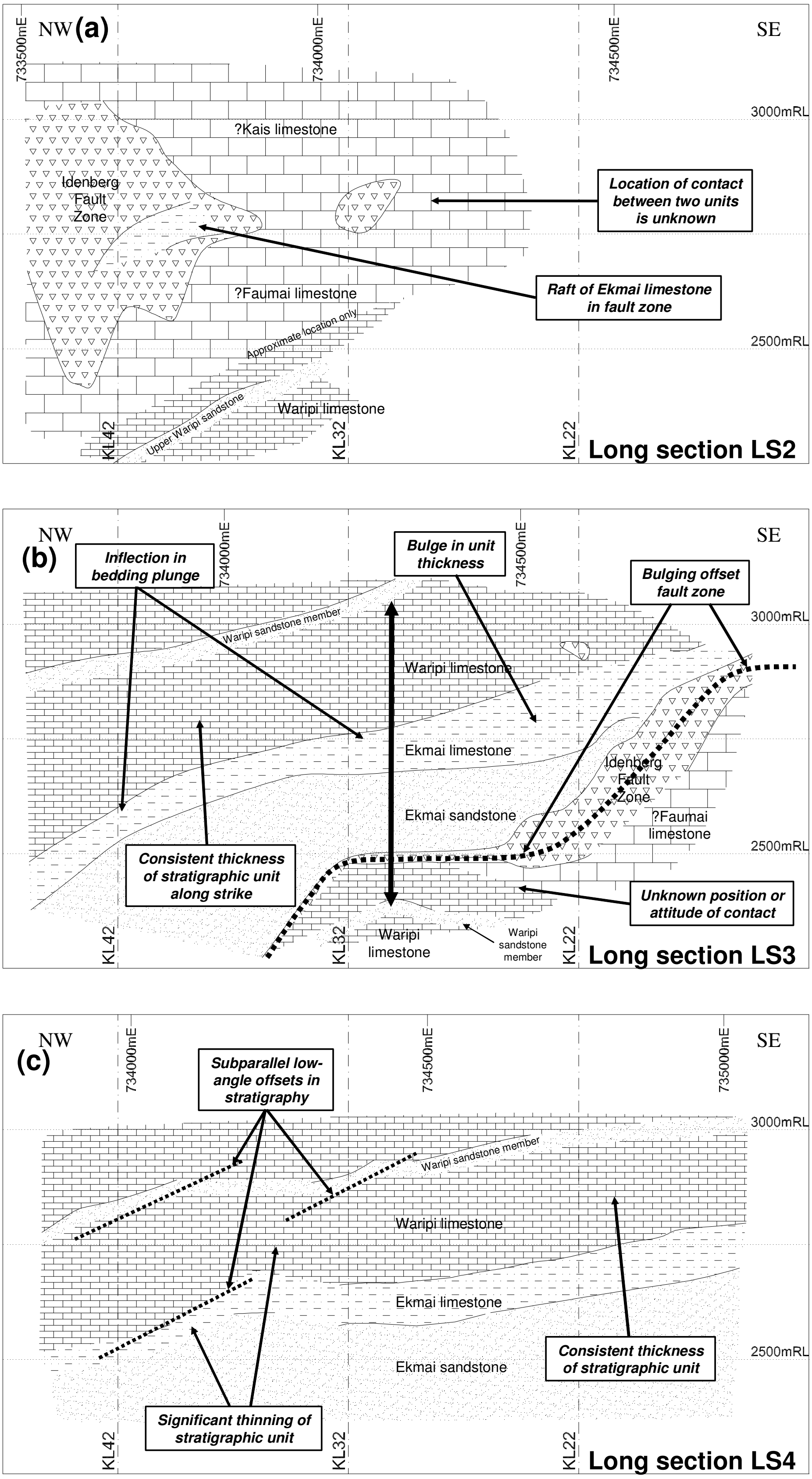

Three representative long sections of the stratigraphic wireframes created from 3D drilling data. Intersections of stratigraphic wireframes with the section plane are indicated by continuous lines. The sections are vertical and orientated perpendicular to the primary drilling azimuth (see Figure 4-3 and 4-4). (a) Is generally in the footwall of the Idenberg Fault Zone (IFZ) which can be seen in the far left of the section. (b) A section through the middle of the deposit shows thickening of the Ekmai Limestone as well as a bulging offset in the IFZ which is not equivalent to that observed in cross sections in Figure 4-3. The total displacement across the IFZ is indicated by a thick double-headed arrow. (c) A section close to the GIC (see Figure 4-3) shows relatively simple stratigraphy with minor offsets and thinning.

4.1.2 Hydrothermal mineral distribution

This section covers the local-scale controls on fluid infiltration as well as the deposit-scale controls. The structural controls of fluid flow within Kucing Liar are analysed via meso- (hand sample), macro- (single drill hole) and mega-scale (drill fan) patterns of hydrothermal mineral development. Local controls are determined by down hole plots of mineral abundance and lithological data while deposit-scale controls are identified by comparing alteration distribution models with lithological models presented in the previous section.

Patterns of hydrothermal alteration

Fluid flow was not uniform through Kucing Liar wall rocks, as fluids were structurally controlled at various scales. The patterns of mineral distribution are illustrated by down hole logs which display the abundances of each hydrothermal mineral (Figure 4-6). The three examples shown illustrate respectively, the Idenberg fault zone in relatively unaltered hosts (KL32-01), a complex fault system and complicated stratigraphy (KL32-04), and a simple fault system accompanied by simple stratigraphy (KL32-05). KL32-01, KL32-04 and KL32-05 were all drilled toward 219º at 0, 45 and 60º respectively. In KL32-01, sedimentary rocks on the north side of the fault are generally unaltered except for low abundance calcite ± magnetite alteration of the upper Waripi sandstone member that elsewhere commonly contains quartz alteration. KL32-04 was drilled at -45° and intersected two fault zones delineated by zones where the lithology is generally unrecognisable. KL32-05 was drilled at a steeper angle and intersected deeper sections of the Idenberg Fault Zone. Discrete intersections dominated by single minerals extend in length from 5-100m along a drill hole and are commonly 10-20m. Contacts between such zones dominated by different minerals are commonly sharp. Some exceptions include gradual and sympathetic abundance changes between K-feldspar and quartz alteration in the Ekmai Limestone (KL32-04, 350-400m). However, contacts of the K-feldspar-quartz with magnetite-sulphide and clinopyroxene are commonly sharp.

Figure 4-6 Lithological patterns and mineral abundances in representative drill holes

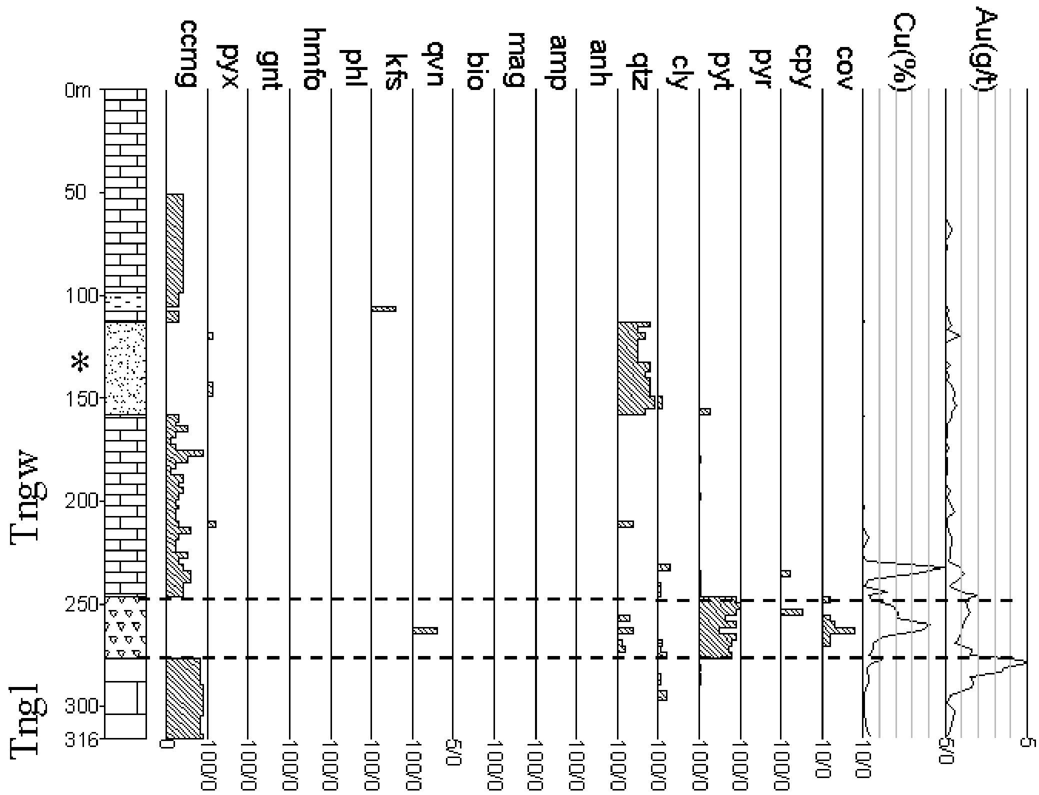

KL32-01 Idenberg Fault in relatively unaltered hosts

This figure is intended to demonstrate three patterns of lithology and alteration encountered in drilling conducted on the same cross section (KL32). See Figure 1-12 for the precise angular relationships between each drillhole. Ornamentation is based on identified lithology while the unit codes are interpreted based on sequence of lithology. See Appendix V for mineral abbreviations and details of logging process. Stratigraphic unit codes are; Tngw = Waripi Limestone, Tngl = undifferentiated New Guinea Limestone Group limestone, Kkel = Ekmai Limestone, Kkes = Ekmai Sandstone. Dashed lines mark the upper and lower boundaries of unrecognised lithologies that are interpreted to represent fault zones. An asterisk is used to identify the location of the upper Waripi sandstone member, which is used to establish the total vertical offset.

Figure 4-6 (cont.)

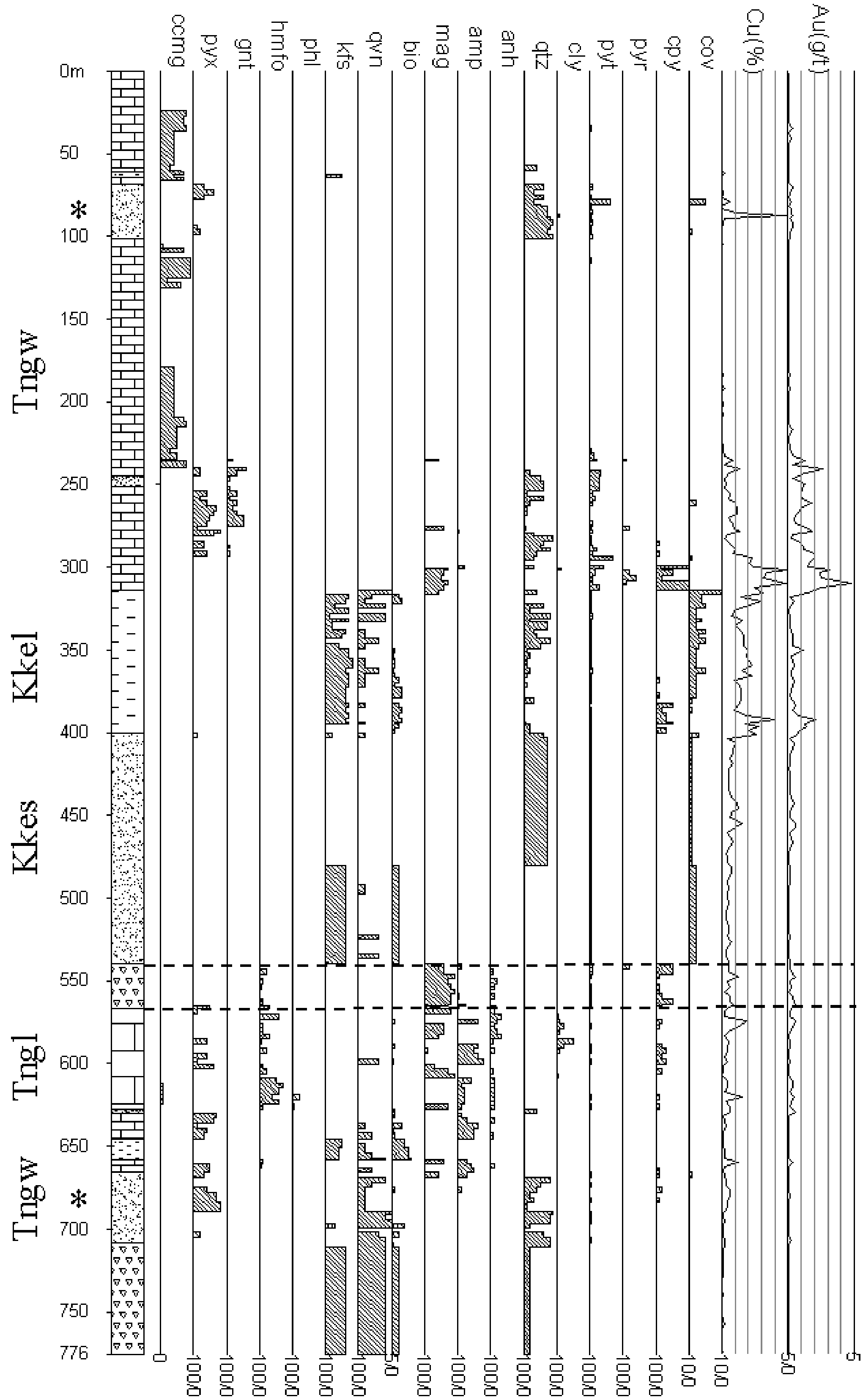

KL32-05 Simple faulted stratigraphic sequence

Figure 4-6 (cont.)

KL32-04 Complex fault and offset stratigraphy

Large-scale mineral distributions

Clinopyroxene ± garnet skarn (see Chapter 3) is developed as thick (~20-50m-scale) lenses in the lower Waripi Limestone and Ekmai Limestone, parallel to the folded stratigraphy and are apparently truncated up dip by the Idenberg Fault Zone (Figure 4-7). Bodies with moderate to high preserved abundances of skarn-related minerals form a series of stacked lenses that occupy the lower Waripi and Ekmai Limestones, paralleling the bedding (Figure 4-7). Semi-concordant skarn rocks in the southeast of the deposit are concentrated in the lower Waripi Limestone and subordinate positions in the Ekmai Limestone (Figure 4-7). Skarn alteration does not persist to the northwest past the apparent truncation and thinning of the Ekmai Limestone (Figure 4-7). Early skarn is zoned with garnet occupying the primary channelways surrounded by clinopyroxene (*cf.* small-scale features illustrated in Section 3.2.1). Similarly, a large skarn body dominated by garnet occurs within the Idenberg Fault Zone. Skarn alteration maintains a constant thickness of 50m for 500m along strike, and maintains a constant position 50m above the base of the Waripi Limestone. The low density of data in these regions did not allow confident constructions of volumetric models for skarn mineral development in the footwall sequence to the southwest of the Idenberg Fault Zone.

Volumes of preserved moderate abundances of K-feldspar ± biotite are tightly restricted to the Ekmai Limestone (Figure 4-8). In cross section, K-feldspar ± biotite rocks are concentrated wholly within the Ekmai Limestone. Biotite alteration is most extensive where the Ekmai Limestone is thickest but is also concentrated in deeper portions of the Ekmai Sandstone and associated with the Idenberg Fault Zone (Figure 4-8). By contrast, moderately magnetite-rich rocks are prominent as a single concentration 20m thick along the base of the Waripi Limestone, extending along most of the identified strike extent (Figure 4-9). Significantly, the magnetite rocks extend into the Grasberg Igneous Complex where they appear to be portioned at the Grasberg Igneous Complex boundary, the first alteration to appear as such (Figure 4-9). At the deepest levels in the down-faulted stratigraphic package, magnetite is concentrated in limestone, assumed to be Faumai Limestone, above the upper Waripi sandstone member (Figure 4-9).

Retrograde skarn minerals tremolite-actinolite and serpentine have a similar distribution to magnetite, though details of any stratigraphical or structural control are not visible.

Quartz alteration is concentrated into stratigraphic layers abutting the Idenberg Fault Zone (Figure 4-10). Well-defined bodies of quartz-dominant material 10-50m thick were identified in drill core and are found to extend up to 500m along strike (Figure 4-10). Quartz alteration is less well developed in the east than in the west. Quartz alteration also occurs as a discrete package in the upper Waripi sandstone member. Moderate to high abundances of sulphides are concentrated within the Idenberg Fault Zone (i.e. broadly coincident with quartz alteration) (Figure 4-11). Additional smaller concentrations of sulphides are present along major stratigraphic contacts, particularly the Ekmai Limestone contacts. Sulphide concentrations are continuous for hundreds of metres along strike (Figure 4-11). Sulphide development is not continuous from the Idenberg Fault Zone to the Grasberg Igneous Complex. The independent development of chalcopyrite and covellite-bearing mineralisation is reconfirmed in models of their spatial distribution (Figure 4-11). Distributions of covellite-bearing mineralisation are distinctly concentrated about the Idenberg Fault Zone as well as in the adjacent Ekmai Limestone. In contrast, chalcopyrite-bearing mineralisation is concentrated along the Ekmai Limestone and is continuous into the Grasberg Igneous Complex.

Figure 4-7 Distribution of calcite, clinopyroxene, garnet, humite and phlogopite

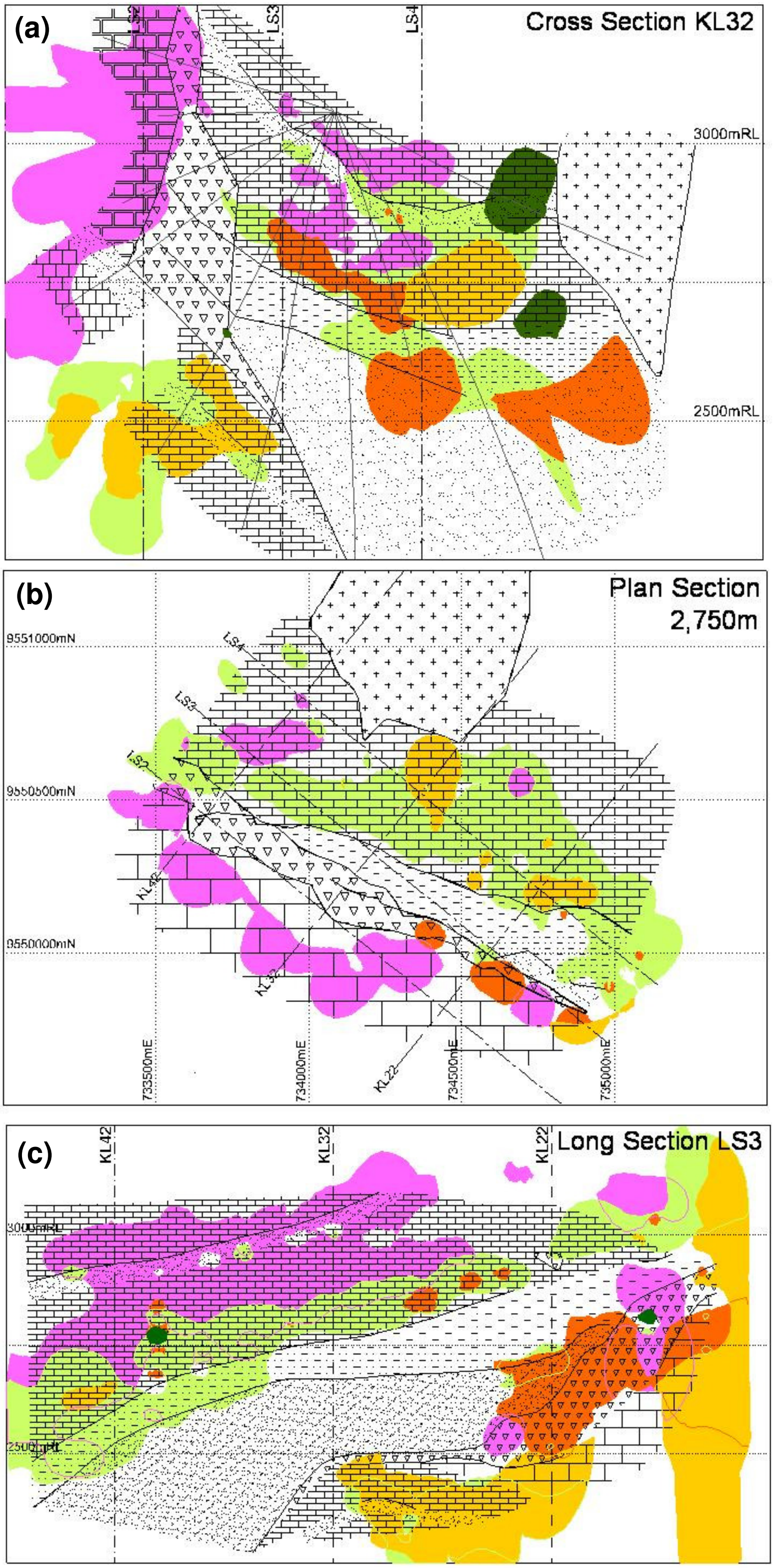

Sections of skarn alteration differentiated by the various minerals identified in Chapter 3. The Grasberg contact was provided by Freeport geologists.

(a) A cross section through station KL32 shows the stratiform nature due to lithological layer control of clinopyroxene and garnet accumulations as well as zoning pattern of garnet inside clinopyroxene. (b) A plan section through 2,750m demonstrates that the skarn development does not envelop the GIC. The asymmetric zoning of skarn across the IFZ relative to elevation is also clear. (c) A long section perpendicular to cross sections demonstrates once more the stratiform nature of skarn as well as the zoning pattern grading from proximal garnet to clinopyroxene to distal calcite ± magnetite. See (a) & (b) for location.

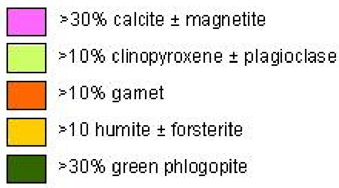

Figure 4-8 Distribution of dominant K-feldspar + biotite alteration

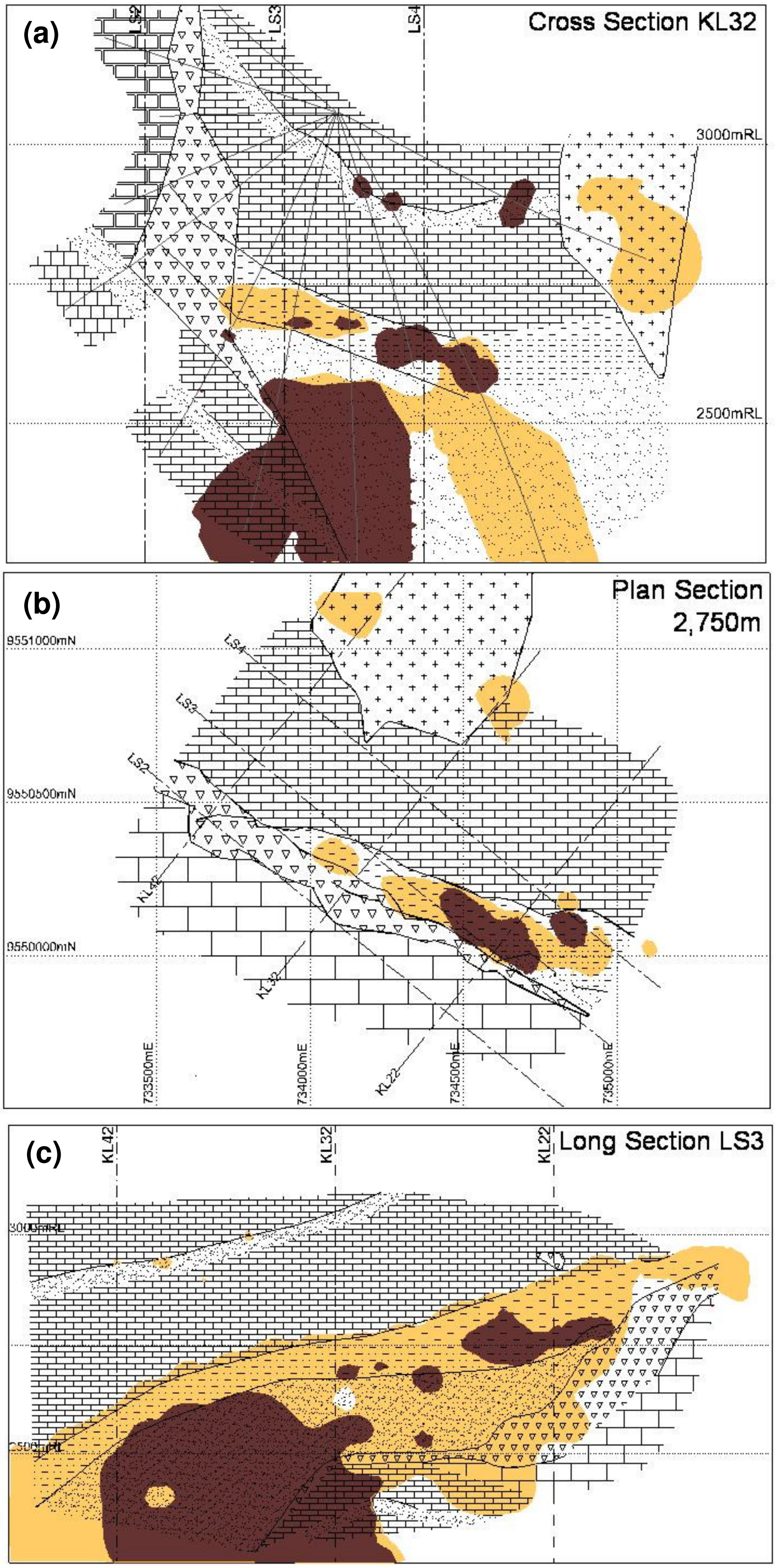

Sections of the distributions of the various potassic alteration group minerals identified in Chapter 3. The Grasberg contact was provided by Freeport geologists.

(a) A cross section through station KL32 shows the stratiform nature due to lithological layer control of K-feldspar and biotite accumulations. Deeper sections of Kucing Liar are biotite rich about the IFZ. (b) A plan section through 2,750m demonstrates the lithological control as well as a suggestion of zoning from inboard biotite to more distal K-feldspar. (c) A long section perpendicular to cross sections demonstrates once more the lithological control highlighted in Chapter 3 as well as the zoning pattern grading from proximal biotite to more distal K-feldspar. See (a) & (b) for location.

Figure 4-9 Distribution of extensive magnetite and tremolite-actinolite alteration

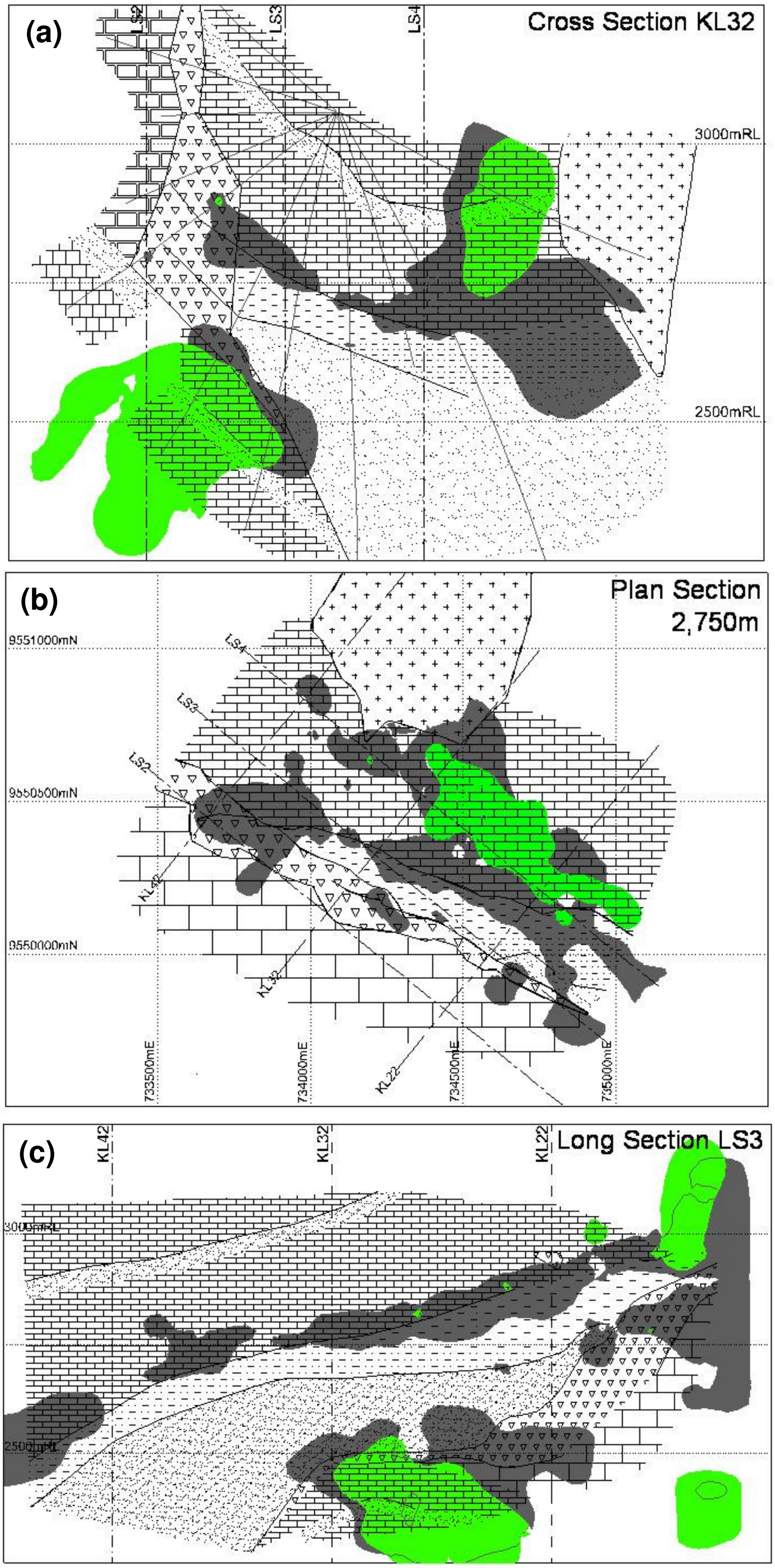

Sections of the distributions of magnetite and retrograde skarn alteration identified in Chapter 3 demonstrate the strong lithological (or stratigraphic contact) control on magnetite and retrograde skarn and also that retrograde skarn and some magnetite is not stratiform. The Grasberg contact was provided by Freeport geologists.

(a) A cross section through station KL32 shows that a large amount of magnetite is juxtaposed with the GIC. The section demonstrates a hydrothermal connection between the GIC and Kucing Liar during magnetite alteration (b) A plan section through 2,750m demonstrates the same connectivity with the GIC. (c) A long section perpendicular to cross-sections demonstrates once more the strong stratigraphical control. See (a) & (b) for location.

Figure 4-10 Distribution of rocks dominated by quartz, muscovite and anhydrite alteration

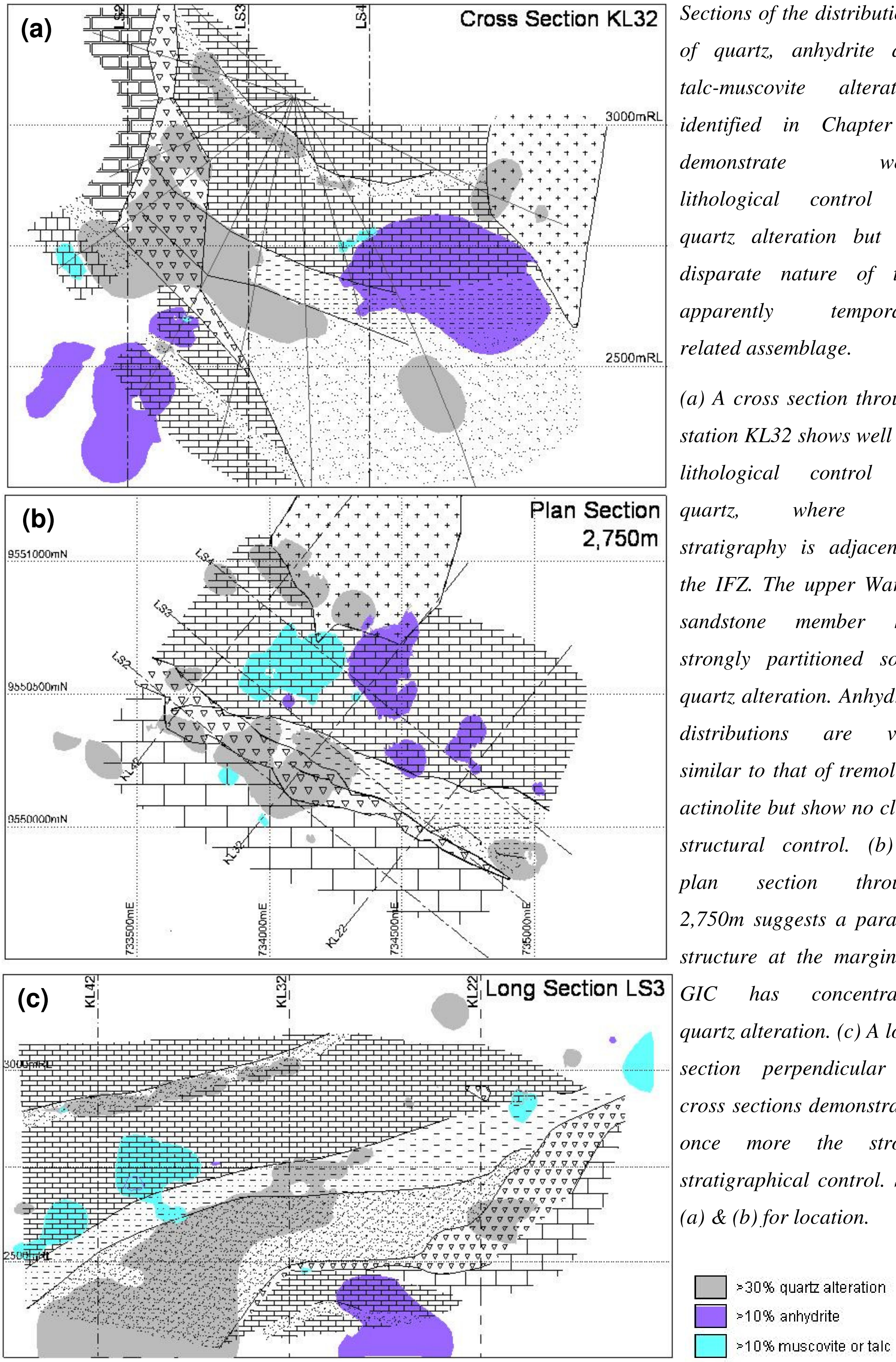

Sections of the distributions of quartz, anhydrite and talc-muscovite alteration identified in Chapter 3 demonstrate weak lithological control on quartz alteration but the disparate nature of this apparently temporally related assemblage.

(a) A cross section through station KL32 shows well the lithological control on quartz, where the stratigraphy is adjacent t the IFZ. The upper Waripi sandstone member has strongly partitioned some quartz alteration. Anhydrite distributions are very similar to that of tremolite-actinolite but show no clear structural control. (b) A plan section through 2,750m suggests a parallel structure at the margin of GIC has concentrated quartz alteration. (c) A long section perpendicular to cross sections demonstrates once more the strong stratigraphical control. See (a) & (b) for location.

Figure 4-11 Distribution of ore sulphides, pyrite, chalcopyrite and covellite

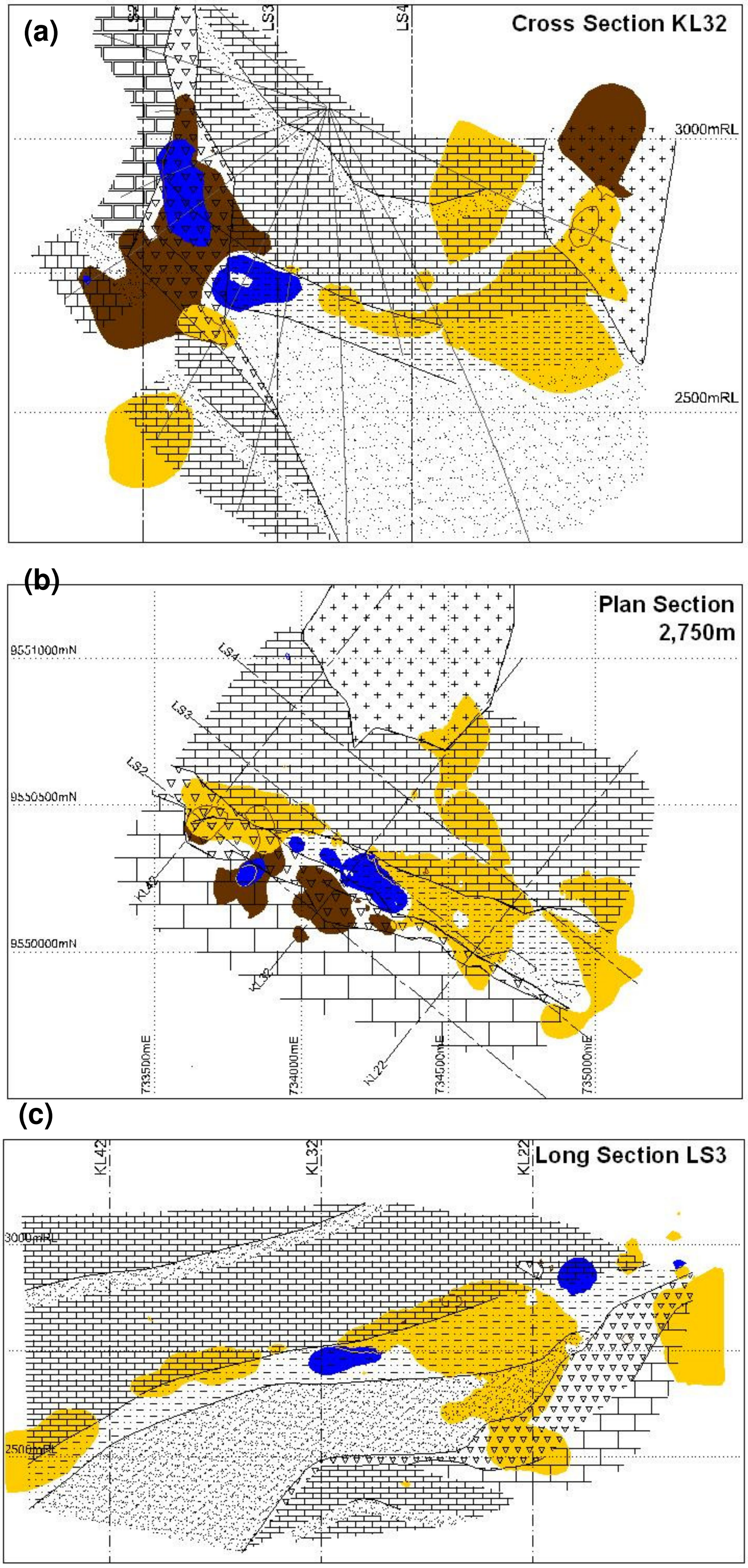

Sections of the distributions of pyrite, chalcopyrite and covellite demonstrate the strong influence of the IFZ and more subtle lithological control on ore minerals as well as a zoning pattern about the IFZ of proximal covellite and distal chalcopyrite.

(a) A cross section through station KL32 shows the intensity of pyrite and covellite development in the IFZ offset as well as the influence of the Ekmai Limestone. (b) A plan section through 2,750m shows the most intense pyrite alteration is opposite the GIC. Note that the contact zone of Kucing Liar and the GIC where magnetite and retrograde skarn are concentrated is occupied by high chalcopyrite concentrations. (c) A long section perpendicular to cross sections further demonstrates the zoning pattern of ore minerals. See (a) & (b) for location.

4.2 LARGE-SCALE CONTROLS ON FLUID INFILTRATION

The data in this chapter will show that the Kucing Liar hydrothermal system was related to a major structural offset in the Idenberg Fault Zone, which is adjacent to a significant lithological contrast.

4.2.1 Structural geometry of Kucing Liar alteration

The combination of specific rock types and marker horizons (Chapter 2) has enabled construction of a lithological model for the mineralised zone. Models of these data indicate that Kucing Liar lies within the north dipping limb of a syncline, although no fold closures are evident in the study area. Adjacent to the Grasberg Igneous Complex the bedding is folded against the intrusion contact, suggesting forceful intrusion. The host stratigraphy has been truncated at a very shallow angle to strike by a steeply dipping fault zone. The fault zone is named the Idenberg Fault Zone and contains several steeply northeast dipping narrow structures that are connected by wide zones of brecciation. The zone of displacement follows both the narrow structures and wide zones to produce a series of offsets within the fault zone. The displaced portion of Kucing Liar on the southwest of the Idenberg Fault Zone is difficult to analyse due to very low data densities. The same rock types are encountered in the footwall of the Idenberg Fault Zone, though skarn is more prevalent than other alteration types.

The mineral distribution data indicate the Idenberg Fault Zone focussed the entire system while a series of complex offsets in the fault zone provided local controls, specifically on garnet and sulphide distributions. Specific alteration assemblages are concentrated along the lower Waripi and Ekmai Limestone contacts, as well as within the Idenberg Fault Zone, especially within offsets of the fault. Within the mineralised zone hydrothermal alteration occupies the upper sandstone member of the Waripi Limestone, the lower Waripi Limestone, the Ekmai Limestone and also extends downwards into the Ekmai Sandstone. Skarn alteration tends to be stratiform and is concentrated in the Ekmai Limestone and lower half of the Waripi Limestone. Humite-forsterite

± serpentine and clinopyroxene ± tremolite-actinolite are restricted to the dolomitic Waripi Limestone (see Chapter 2) within the main mineralised zone and appear to stratiform and interlayered, perhaps reflecting the original distribution of dolomite and calcite in the limestone unit. Garnet and magnetite are localised within the Waripi Limestone along its lower contact with the Ekmai Limestone and to a lesser extent along the base of the Ekmai Limestone. Small concentrations of garnet are also localised along the upper skarn contact within the Waripi Limestone. K-feldspar ± biotite, along with related quartz veins, is generally restricted to the Ekmai Limestone and Ekmai Sandstone though biotite also formed independently within narrow portions of the Idenberg Fault Zone below the elevation of the main mineralised zone. Quartz and sulphide alteration have very similar distributions that appear to parallel the steeply dipping structures within the Idenberg Fault Zone and are concentrated about a large-scale offset in the fault zone. Quartz and sulphide are structurally distinct from other alteration assemblage, as they do not form large stratiform bodies. The change in alteration distribution from skarn to potassic to silica-pyrite indicates a change in structural controls that will be analysed in the next section. The relationship between chalcopyrite and covellite mineralisation in Kucing Liar and the Grasberg porphyry system has not been comprehensively tested, though the two systems have similar ore assemblages, there are some grounds for believing the two are distinct systems, and will be further discussed in Chapter 9.

The data indicate mineralisation that is zoned with respect to fluid flow. Mertig *et al.,* (1994), Hefton *et al.*, (1995), and Rubin and Kyle (1998) have described vertical zonation of alteration and mineralisation in the magnesian skarn deposits of the EESS, formally referred to as GBT-IOZ-DOZ (see Chapter 1). The focus of fluid flow at Kucing Liar was the Idenberg Fault Zone, and in particular offset within it, and fluids probably flowed upwards and along stratigraphic contacts to that feature. Fluids may then have migrated within the Idenberg Fault Zone to higher elevations. In a model where covellite formation is at least partly contemporaneous with, though spatially distinct from, chalcopyrite, the data suggest that chalcopyrite ± pyrite was accompanied by and locally overprinted by covellite ± pyrite, which is restricted to the high flow areas. Both of these forms of copper mineralisation were replaced in the core of the Idenberg Fault Zone by a package of pyrite ± chalcopyrite ± covellite. Pyrite, chalcopyrite and covellite core are overprinted by galena and sphalerite.

4.2.2 Driving forces of fluid flow

Fluid infiltration through rocks may be via primary or secondary porosity. Primary porosity is a function of the grain size, degree of cementation and distribution of the wall rocks, while secondary porosity is that which is created during deformation or alteration in the absence of deformation. The very fine-grained texture of rock samples, particularly pyroxene and feldspar, indicate derivation from rapid deposition at numerous nucleation sites, which can result from high fluid fluxes that are conducive to supersaturation (Einaudi *et al.*, 1981). Additionally, pervasive fluid flow such as is observed to have occurred during skarn and potassic (K-feldspar ± biotite) alteration is inferred to occur along microcracks and grain-boundary porosity (Oliver, 1996). Pervasive fluid flow produces uniform replacement of wall rocks, referred to as penetrative alteration (Chapter 3). Widespread penetrative alteration is indicative of low fluid pressures and will typically be associated with relatively high fluid fluxes as compared to channelled flow (Oliver, 1996). Channelled fluid flow occurs along fractures in wall rocks but is accompanied by substantial infiltration into the local wall rocks, typically resulting in a mineralogical selvedge (Oliver, 1996). The progressively declining scales of penetrative alteration accompanied by increased fracture selvedge and infill indicate that fluid flow became more and more channelled accompanied by increasing fluid pressures. There are also indications that the amount of channelled fluid flow increased with time, evidenced by the increase in infill relative to alteration and the decrease in penetrative alteration in later stages of the paragenesis (Chapter 3).

Within a fault zone, fluid migration occurs from zones of high interstitial pressure and high strain (contraction zone) to zones of low interstitial pressure (dilation zone) (Guha et al., 1983). Flow localization within faults and shear zones occurs in areas of highest fracture aperture and fracture density, such as damage zones associated with fault jogs, bends and splays (Cox *et al.*, 2001).

Offsets are thus favourable sites for fluid flow due to complex geometry created by the large amount of wall rock partings and intersections of variably oriented fractures. Fluid flow in a fault network is governed by creation of permeability through movement. Where high fluid pressures produce low effective confining pressures, grain scale crack growth significantly increases the permeability of the active shear zone relative to their host rocks (Cox et al., 2001). Thus, secondary permeability is created by high pore fluid pressure regimes, which favour fracture growth (Cox *et al.*, 2001). Mineral-filled fractures in hydrothermal systems indicate tensile effective stress states, and thus, fluid pressures greater than $\sigma 3$ (lithostatic load) (Cox *et al.*, 2001). Sustained hydrothermal flow must be accompanied by repetitive and continued wall rock fracturing given that mineral sealing is rapid compared to the lifetimes of hydrothermal systems (Cox *et al.*, 2001). Consequently, sustained fluid flow occurs only in active structures where permeability is repeatedly renewed. Fault motion is accommodated by earthquake-related rupturing (Sibson, 2001) and is accompanied by significant fluid redistribution that occurs throughout the aftershock phase following large earthquakes (Cox et al., 2001). Secondary porosity related to lithological layering may also be produced during folding as deformation of heterogeneous rocks creates dilatancy due to competency contrast, as well as large variations in pore fluid pressure (P_f), leading to brecciation along these contacts (Oliver *et al.*, 2001).

Thus deformation can explain brecciation along the base of the Waripi Limestone. In similar fashion to Kucing Liar, the Big Gossan deposit is concentrated in breccia bodies within the lower Waripi Limestone near the contact with the Ekmai Limestone, which was altered to pyroxene-feldspar and biotite-feldspar hornfels and also contains local garnet-pyroxene skarn (Meinert et al., 1997). The preference for the Ekmai Limestone as a host for quartz vein arrays may also be derived from ground preparation due to contact metamorphism of the shaly limestone, as brittle calc-hornfels are easily fractured during deformation (Einaudi *et al.*, 1981).